

Brown adipose tissue in a newborn

Brett W. Carter, MD, and William G. Schucany, MD

A premature infant boy of 35 weeks and 4 days weighing 2605 g was found to have bilateral supraclavicular masses at 13 days of life. He had persistent pulmonary hypertension of the newborn and thrombocytopenia. Delivery was by cesarean section for nonreassuring fetal status, and Apgar scores were 5 at 1 minute and 8 at 5 minutes.

Initial radiographs of the chest demonstrated abnormal supraclavicular fullness bilaterally (*Figure 1*), and soft tissue neck sonography demonstrated hyperechoic masses involving the supraclavicular region bilaterally with internal vascular flow and hyperechoic bands. Differential considerations included lipoma, lipofibroma, hemangioma, and lymphangioma.

Computed tomography (CT) of the chest and neck were subsequently performed to evaluate the masses for the presence of fat (*Figure 2*). Hypodense masses were demonstrated within the axilla, supraclavicular fossa, and lower neck bilaterally. Peripheral nodular enhancement was present within the axillae. Differential considerations included mixed venolymphatic malformation, heman-gioma, and lympho-proliferative disorder. There was no evidence of lymphadenopathy within the chest or neck.

Subsequent mag-netic resonance imag-ing (MRI) of the chest demonstrated symmet-ric and confluent soft tissue extending from

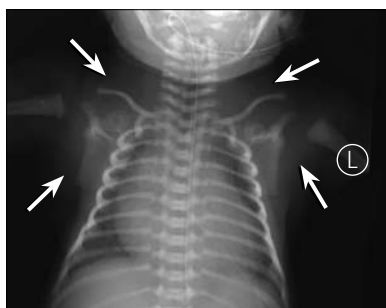


Figure 1. Chest radiograph demonstrates supraclavicular and axillary “fullness” and fatty density (*arrows*).

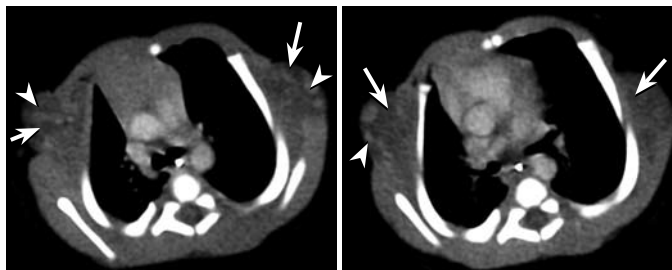


Figure 2. CT of the chest demonstrates bilateral fat density (*arrows*) with nodular enhancement (*arrowheads*) in the axilla and along the lateral chest.

the neck inferiorly to the chest (*Figure 3*). This soft tissue demonstrated intermediate signal intensity and was homogeneously isointense to muscle on T1-weighted images. This tissue was homogeneously hyperintense to muscle and hypointense to fat on T2-weighted images.

What is the most likely diagnosis?



Figure 3. MRI images of the chest and neck. (**a**) Coronal T2-weighted image demonstrates a bilateral symmetric supraclavicular and axillary confluent mass (*arrows*). (**b**) Axial T1-weighted image demonstrates bilateral symmetric intermediate signal intensity mass at mid chest level (*arrows*). (**c**) Axial T1-weighted image demonstrates bilateral intermediate signal intensity mass in the lower neck (*arrows*). (**d**) Axial T2-weighted image at mid chest level demonstrates bilateral intermediate signal intensity soft tissue (*arrows*) with nodular hyperintensity (*arrowhead*). (**e**) Axial T2-weighted image at lower neck level demonstrates bilateral symmetric intermediate signal intensity mass (*arrows*).

From the Department of Radiology, Baylor University Medical Center, Dallas, Texas.

Corresponding author: William G. Schucany, MD, Department of Radiology, Baylor University Medical Center, 3500 Gaston Avenue, Dallas, Texas 75246 (e-mail: gschucany@americanrad.com).

DIAGNOSIS: Brown adipose tissue (BAT).

DISCUSSION

BAT is one of two types of adipose tissue that is found in the human body, the other being white adipose tissue. The tissue has been previously described in hibernating animals. Thus, the term *hibernoma* has been given to benign tumors of BAT. BAT derives its name from its gross appearance, the brown color attributed to its extensive vascularity and proportion of mitochondria. The mitochondria present within BAT are responsible for its characteristic cold-induced and diet-induced thermogenesis by expressing uncoupling protein-1 (UCP1). UCP1 ultimately results in the dissipation of heat by uncoupling oxidative respiration from the production of adenosine triphosphate, resulting in a compensatory increase in glucose metabolism by anaerobic glycolysis (1). Although many classical growth factors such as fibroblast and insulin-like growth factors are influential in the activity of brown adipocytes, norepinephrine has a primary role in determining the acute rate of thermogenesis and the degree of recruitment. These actions are largely based on the direct regulation of UCP1 by norepinephrine (2).

BAT typically accumulates within the neck, axillae, back, mediastinum, abdomen, and thigh and is more profuse in the fetus and neonate, in whom it constitutes approximately 5% of body weight. BAT is involved in nonshivering thermogenesis when the body temperature falls below a threshold value and serves as cushioning and protection for vital body parts such as major blood vessels and mediastinal structures (3).

BAT is an important entity and potential pitfall with regards to nuclear medicine imaging, as the tissue has demonstrated radiotracer uptake with ^{18}F -fluoro-deoxy-glucose (^{18}F -FDG), $^{99\text{m}}\text{Tc}$ -methoxyisobutylisonitrile, $^{99\text{m}}\text{Tc}$ -tetrofosmin, and ^{123}I -meta-iodobenzylguanidine (4). ^{18}F -FDG uptake within the neck and supraclavicular regions has been described with positron emission tomography (PET) imaging and had previously been attributed to muscle activity because uptake was no longer demonstrated after the administration of muscle relaxants (5). Hypermetabolic BAT expresses glucose transporters, enabling the uptake of FDG after administration. Whereas radiotracer uptake in the supraclavicular region demonstrates a classic imaging appearance, uptake by BAT within the chest and mediastinum may be mistaken for malignancies and lymphadenopathy. By precisely localizing ^{18}F -FDG uptake, fusion PET/CT can be used to distinguish radiotracer uptake by different tissues such as BAT and malignancies (6).

On CT, BAT is intermediate in attenuation between fat and muscle and demonstrates enhancement with some washout on delayed imaging. BAT has been described as minimally hyperintense to muscle on T1-weighted images and heterogeneously hyperintense to muscle on T2-weighted images, with maintenance of hyperintensity on chemical fat-suppressed T2-weighted images and some loss of signal on fat-suppressed T1-weighted images (7).

The primary differential considerations on imaging studies include hibernomas, lipomas, and soft tissue tumors of infancy

such as rhabdomyosarcomas, the fibromatoses, and heman-giomas.

Hibernomas are benign neoplasms composed almost entirely of BAT that chiefly affect patients in the fourth and fifth decades of life (8). The typical presentation is that of a slow and painlessly enlarging, well-defined and encapsulated mobile mass. MRI demonstrates well-circumscribed masses whose signal intensity is intermediate between subcutaneous fat and muscle on all pulse sequences. CT demonstrates enhancement after the administration of intravenous contrast. Hibernoma can usually be differentiated from BAT by the presence of a discrete mass (9).

Lipomas present as predominantly fatty masses. On MRI, lipomas appear as encapsulated masses whose signal intensities are similar to those of subcutaneous fat on all pulse sequences. The nonadipose portions of these masses demonstrate T1 hypointensity and various signal intensities on the T2-weighted images (10).

Rhabdomyosarcomas, of which the most common type to afflict infants is embryonal, tend to develop after several months of life and appear as discrete masses involving striated muscle on imaging studies (11).

The most common of the fibromatoses to affect infants is infantile myofibromatosis, which typically affects the skeleton, lungs, heart, and gastrointestinal tract. The fibromatoses demonstrate soft tissue attenuation on CT. On MRI, the masses are isointense to minimally hyperintense to muscle on T1-weighted images and either isointense to subcutaneous fat or intermediate in intensity between subcutaneous fat and muscle on T2-weighted images (12).

Hemangiomas may be seen in the early neonatal period and are associated with bluish discoloration of the overlying skin. These masses are typically isointense to muscle on T1-weighted images, hyperintense on T2-weighted images, and demonstrate flow voids (13).

In this patient, a biopsy of the mass within the left aspect of the neck was subsequently obtained and showed adipose tissue, some of which was necrotic. On the MRI of the chest, intracranial hemorrhage was partially visualized, and subsequent MRI of the brain demonstrated grade IV intraventricular hemorrhage, intraparenchymal hemorrhage centered within the right parietal lobe, and a thin right posterior fossa subdural hematoma. Over the next 8 days, the masses gradually became smaller, and they were nearly undetectable by the time of discharge.

1. Hany TF, Gharehpapagh E, Kamel EM, Buck A, Himms-Hagen J, von Schulthess GK. Brown adipose tissue: a factor to consider in symmetrical tracer uptake in the neck and upper chest region. *Eur J Nucl Med Mol Imaging* 2002;29(10):1393–1398.
2. Cannon B, Nedergaard J. Brown adipose tissue: function and physiological significance. *Physiol Rev* 2004;84(1):277–359.
3. Evans KD, Tulloss TA, Hall N. ^{18}F FDG uptake in brown fat: potential for false positives. *Radiol Technol* 2007;78(5):361–366.
4. Goetze S, Lavery WC, Ziessman HA, Wahl RL. Visualization of brown adipose tissue with $^{99\text{m}}\text{Tc}$ -methoxyisobutylisonitrile on SPECT/CT. *J Nucl Med* 2008;49(5):752–756.
5. Barrington SF, Maisey MN. Skeletal muscle uptake of fluorine-18-FDG: effect of oral diazepam. *J Nucl Med* 1996;37(7):1127–1129.

6. Truong MT, Erasmus JJ, Munden RF, Marom EM, Sabloff BS, Gladish GW, Podoloff DA, Macapinlac HA. Focal FDG uptake in mediastinal brown fat mimicking malignancy: a potential pitfall resolved on PET/CT. *AJR Am J Roentgenol* 2004;183(4):1127–1132.
7. Dundamadappa SK, Shankar S, Danrad R, Singh A, Vijayaraghavan G, Kim Y, Perugini R. Imaging of brown fat associated with adrenal pheochromocytoma. *Acta Radiol* 2007;48(4):468–472.
8. Furlong MA, Fanburg-Smith JC, Miettinen M. The morphologic spectrum of hibernoma: a clinicopathologic study of 170 cases. *Am J Surg Pathol* 2001;25(6):809–814.
9. da Motta AC, Tunkel DE, Westra WH, Yousem DM. Imaging findings of a hibernoma of the neck. *AJNR Am J Neuroradiol* 2006;27(8):1658–1659.
10. Drevelegas A, Pilavaki M, Chourmouzi D. Lipomatous tumors of soft tissue: MR appearance with histological correlation. *Eur J Radiol* 2004;50(3):257–267.
11. Srinath G, Cohen M. Imaging findings in subcutaneous fat necrosis in a newborn. *Pediatr Radiol* 2006;36(4):361–363.
12. Patrick LE, O’Shea P, Simoneaux SF, Gay BB Jr, Atkinson GO. Fibromatoses of childhood: the spectrum of radiographic findings. *AJR Am J Roentgenol* 1996;166(1):163–169.
13. Norton KI, Som PM, Shugar JM, Rothchild MA, Popper L. Subcutaneous fat necrosis of the newborn: CT findings of head and neck involvement. *AJNR Am J Neuroradiol* 1997;18(3):547–550.